PHYSICAL REVIEW A VOLUME 10, NUMBER 6 DECEMBER 1974

Multiplet effects on the $L_{2,3}$ fluorescence yield of multiply ionized Ar[†] [*]

Mau Hsiung Chen and Bernd Crasemann
Department of Physics, University of Oregon, Eugene, Oregon 97403

(Received 15 July 1974)

The $2p$ fluorescence yield of Ar in the presence of zero to six $3p$ holes has been calculated by statistically averaging the fluorescence yields of initial states that consist of individual multiplet configurations, formed by coupling the $2p$ vacancy to the partially filled $3p$ shell. The $L_{2,3}$ fluorescence yields for the $(2p)^{-1}(3p)^{-n}$ configurations of Ar are found to be 1.48, 17.97, 24.83, 37.84, 79.61, 112.16, and 121.48×10^{-4} for $n = 0$, 1, 2, 3, 4, 5, and 6, respectively. Results agree reasonably well with experimental fluorescence yields deduced from ion-atom collision measurements.

I. INTRODUCTION

We consider an atom that contains an inner-shell vacancy and a partially filled shell, other shells being full. The holes couple so that a multiplet structure results. The width of such multiplet states has recently been discussed by McGuire.[1] Radiationless transition probabilities to different multiplet states can vary substantially.[1,2]

In this paper, we report on calculations of the Ar $2p$ fluorescence yield in the presence of a partially filled $3p$ shell. The fluorescence yield $\omega(LS)$ is computed separately for each initial multiplet state of a given hole configuration $(2p)^{-1}(3p)^{-n}$, and $L_{2,3}$ fluorescence yields are calculated as weighted averages:

$$\bar{\omega}_{2,3} = \frac{\sum_{L,S}\omega(LS)(2L+1)(2S+1)}{\sum_{L,S}(2L+1)(2S+1)} . \qquad (1)$$

Because the various $\omega(LS)$ differ widely, the results differ considerably from $\bar{\omega}_{2,3}$ as calculated traditionally[3,4] from average Auger and radiative widths, each average extending over all multiplet states. It appears that the well-known discrepancy[5,6] between calculated and measured fluorescence yields of atoms with multiple inner-shell vacancies may, at least in some cases, be removed by the approach implicit in Eq. (1).

II. RADIATIONLESS TRANSITIONS

A. $(2p)^{-1}(3p)^{-n} \rightarrow (3p)^{-(n+2)}[L_{2,3}\text{-}M_{2,3}M_{2,3}]$ transitions

McGuire[7] has derived general expressions, in LS coupling, for Auger rates in atoms with arbitrary vacancy structures, and has specialized them[1] for transitions of the type

$$(n_1l_1)[(n_3l_3)^n, \alpha_3 L_3S_3]SL \rightarrow [(n_3l_3)^{n+2}, \beta_3PQ] .$$

The meaning of the subscripts to the quantum numbers is illustrated in Fig. 1; we have $n_3l_3 = n_4l_4$ in the class of transitions considered in this paragraph. The initial multiplet state, with quantum numbers SL, consists of n holes in the n_3l_3 shell, with quantum numbers $\alpha_3L_3S_3$, and one hole in the n_1l_1 shell. The final state consists of $n+2$ holes in the n_3l_3 shell, with quantum numbers β_3PQ. The radiationless transition probability is[8]

$$W_{fi}(LS,PQ) = \tfrac{1}{4}(n+1)(n+2)(2l_3+1)\prod_{i=1}^{3}(2l_i+1)(2P+1)(2Q+1)$$
$$\times \left| \sum_{f,g} (-1)^g[(2f+1)(2g+1)]^{1/2} I(KK'fg) \begin{Bmatrix} \frac{1}{2} & \frac{1}{2} & f \\ S_3 & Q & S \end{Bmatrix} \begin{Bmatrix} l_2 & l_1 & g \\ L_3 & P & L \end{Bmatrix} (l_3{}^{n+2}\beta_3PQ\{|l_3{}^2fg;\, l_3{}^n\alpha_3L_3S_3) \right|^2 . \qquad (2)$$

The $\left\{\begin{smallmatrix} a & b & c \\ d & e & f \end{smallmatrix}\right\}$ are 6-j symbols. The two-electron coefficients of fractional parentage in Eq. (2) are defined as follows[1]:

$$(l^{n+2}\beta PQ\{|l^2fg;\, l^n\alpha LS) = -[(2f+1)(2g+1)]^{1/2}\sum_{\gamma P'Q'}[(2P'+1)(2Q'+1)]^{1/2}\begin{Bmatrix} L & l & P' \\ l & P & g \end{Bmatrix}$$
$$\times \begin{Bmatrix} S & \frac{1}{2} & Q' \\ \frac{1}{2} & Q & f \end{Bmatrix} (l^{n+2}\beta PQ\{|l^{n+1}\gamma P'Q')(l^{n+1}\gamma P'Q'\{|l^n\alpha LS) , \qquad (3)$$

where the $(l^m\beta PQ\{|l^{m-1}\gamma P'Q')$ are the usual coefficients of fractional parentage.

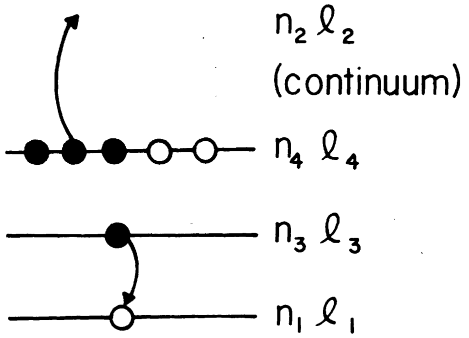

FIG. 1. Schematic representation of a radiationless transition, indicating designation of states. (In the exchange transition, the roles of n_3l_3 and n_4l_4 are interchanged.)

TABLE I. Auger transition probabilities to an initial $2p$ vacancy in an atom with the electron configuration $(1s)^2(2s)^2(2p)^5(3s)^2(3p)^5$, for various initial multiplet states. Results are given in terms of radial integrals $R_K(l_1l_2l_3l_4)$ as defined in Eq. (8).

Multiplet state	Auger transition probability
^1S	$\frac{1}{9}R_1(1100)^2+8R_0(1111)^2-\frac{16}{5}R_0(1111)R_2(1111)$ $+\frac{8}{25}R_2(1111)^2+\frac{1}{9}R_1(1001)^2-\frac{4}{3}R_1(1001)R_0(1010)$ $+4R_0(1010)^2+\frac{2}{9}R_1(1201)^2-\frac{8}{15}R_1(1201)R_2(1210)$ $+\frac{8}{25}R_2(1210)^2$
^1P	$\frac{1}{9}R_1(1100)^2+\frac{36}{125}R_2(1111)^2+\frac{9}{125}R_2(1311)^2$ $+\frac{1}{3}R_1(1001)^2+\frac{1}{3}R_1(1201)^2-\frac{2}{5}R_1(1201)R_2(1210)$ $+\frac{6}{25}R_2(1210)^2$
^1D	$\frac{1}{9}R_1(1100)^2+8R_0(1111)^2-\frac{44}{25}R_0(1111)R_2(1111)$ $+\frac{74}{625}R_2(1111)^2+\frac{81}{625}R_2(1311)^2$ $+\frac{19}{45}R_1(1201)^2-\frac{22}{75}R_1(1210)R_2(1210)$ $+\frac{22}{125}R_2(1210)^2+\frac{1}{9}R_1(1001)^2$ $-\frac{4}{3}R_1(1001)R_0(1010)+4R_0(1010)^2$
^3S	$\frac{1}{9}R_1(1100)^2+\frac{1}{9}R_1(1001)^2+\frac{2}{9}R_1(1201)^2$
^3P	$\frac{1}{9}R_1(1100)^2+8R_0(1111)^2-\frac{4}{5}R_0(1111)R_2(1111)$ $+\frac{16}{125}R_2(1111)^2+\frac{9}{125}R_2(1311)^2+\frac{1}{3}R_1(1001)^2$ $-\frac{4}{3}R_1(1001)R_0(1010)+4R_0(1010)^2+\frac{1}{3}R_1(1201)^2$ $-\frac{2}{15}R_1(1201)R_2(1210)+\frac{2}{25}R_2(1210)^2$
^3D	$\frac{1}{9}R_1(1100)^2+\frac{54}{625}R_2(1111)^2$ $+\frac{81}{625}R_2(1311)^2+\frac{1}{9}R_1(1001)^2$ $+\frac{19}{45}R_1(1201)^2-\frac{6}{25}R_1(1201)R_2(1210)$ $+\frac{18}{125}R_2(1210)^2$

TABLE II. Auger transition probabilities to an initial $2p$ vacancy in an atom with the electron configuration $(1s)^2(2s)^2(2p)^5(3s)^2(3p)^4$, for various initial multiplet states. Results are given in terms of radial integrals $R_K(l_1l_2l_3l_4)$ as defined in Eq. (8).

Multiplet state	Auger transition probability
$(^1S)^2P$	$\frac{1}{9}R_1(1100)^2+2R_0(1111)^2+\frac{14}{125}R_2(1111)^2$ $+\frac{6}{125}R_2(1311)^2+\frac{4}{3}R_0(1010)^2$ $-\frac{4}{9}R_0(1010)R_1(1001)+\frac{4}{27}R_1(1001)^2$ $+\frac{8}{27}R_1(1201)^2-\frac{8}{45}R_1(1201)R_2(1210)$ $+\frac{8}{75}R_2(1210)^2$
$(^3P)^2S$	$\frac{1}{9}R_1(1100)^2+\frac{9}{25}R_2(1111)^2+\frac{4}{9}R_1(1001)^2$ $+\frac{2}{9}R_1(1201)^2-\frac{2}{5}R_1(1201)R_2(1210)+\frac{6}{25}R_2(1210)^2$
$(^3P)^2P$	$\frac{1}{9}R_1(1100)^2+\frac{9}{2}R_0(1111)^2-\frac{9}{5}R_0(1111)R_2(1111)$ $+\frac{9}{50}R_2(1111)^2+3R_0(1010)^2-R_0(1010)R_1(1001)$ $+\frac{1}{9}R_1(1001)^2+\frac{2}{9}R_1(1201)^2$ $-\frac{2}{5}R_1(1201)R_2(1210)+\frac{6}{25}R_2(1210)^2$
$(^3P)^2D$	$\frac{1}{9}R_1(1100)^2+\frac{9}{2}R_0(1111)^2-\frac{27}{25}R_0(1111)R_2(1111)$ $+\frac{117}{1250}R_2(1111)^2+\frac{54}{625}R_2(1311)^2+3R_0(1010)^2$ $-R_0(1010)R_1(1001)+\frac{1}{9}R_1(1001)^2$ $+\frac{16}{45}R_1(1201)^2-\frac{8}{25}R_1(1201)R_2(1210)+\frac{24}{125}R_2(1210)^2$
$(^3P)^4S$	$\frac{1}{9}R_1(1100)^2+9R_0(1111)^2+\frac{4}{9}R_1(1001)^2$ $-2R_1(1001)R_0(1010)+6R_0(1010)^2+\frac{2}{9}R_1(1201)^2$
$(^3P)^4P$	$\frac{1}{9}R_1(1100)^2+\frac{1}{9}R_1(1001)^2+\frac{2}{9}R_1(1201)^2$
$(^3P)^4D$	$\frac{1}{9}R_1(1100)^2+\frac{36}{625}R_2(1111)^2$ $+\frac{54}{625}R_2(1311)^2+\frac{16}{45}R_1(1201)^2$ $-\frac{4}{25}R_1(1201)R_2(1210)+\frac{12}{125}R_2(1210)^2+\frac{1}{9}R_1(1001)^2$
$(^1D)^2P$	$\frac{1}{9}R_1(1100)^2+\frac{5}{2}R_0(1111)^2-\frac{3}{5}R_0(1111)R_2(1111)$ $+\frac{73}{1250}R_2(1111)^2+\frac{6}{625}R_2(1311)^2+\frac{5}{3}R_0(1010)^2$ $-\frac{5}{9}R_1(1001)R_0(1010)+\frac{5}{27}R_1(1001)^2$ $+\frac{14}{135}R_1(1201)^2-\frac{14}{225}R_1(1201)R_2(1210)$ $+\frac{14}{375}R_2(1210)^2$
$(^1D)^2D$	$\frac{1}{9}R_1(1100)^2+\frac{9}{2}R_0(1111)^2-\frac{9}{25}R_0(1111)R_2(1111)$ $+\frac{153}{1250}R_2(1111)^2+\frac{36}{625}R_2(1311)^2$ $+\frac{4}{15}R_1(1201)^2-\frac{4}{25}R_1(1201)R_2(1210)$ $+\frac{12}{125}R_2(1210)^2+\frac{1}{3}R_1(1001)^2$ $-R_1(1001)R_0(1010)+3R_0(1010)^2$
$(^1D)^2F$	$\frac{1}{9}R_1(1100)^2+\frac{9}{625}R_2(1111)^2$ $+\frac{522}{4375}R_2(1311)^2+\frac{2}{5}R_1(1201)^2$ $-\frac{6}{25}R_1(1201)R_2(1210)+\frac{18}{125}R_2(1210)^2$

We have

$$I(KK'fg)=\sum_{K} D(K)\begin{Bmatrix} l_1 & l_3 & K \\ l_4 & l_2 & g \end{Bmatrix}+(-1)^{f-g}\sum_{K'} E(K')\begin{Bmatrix} l_1 & l_4 & K' \\ l_3 & l_2 & g \end{Bmatrix}. \tag{4}$$

The terms containing the direct and exchange matrix elements are

$$D(K)=R_K(l_1l_2l_3l_4)\begin{pmatrix} l_1 & K & l_3 \\ 0 & 0 & 0 \end{pmatrix}\begin{pmatrix} l_2 & K & l_4 \\ 0 & 0 & 0 \end{pmatrix}, \tag{5}$$

$$E(K)=R_K(l_1l_2l_4l_3)\begin{pmatrix} l_1 & K & l_4 \\ 0 & 0 & 0 \end{pmatrix}\begin{pmatrix} l_2 & K & l_3 \\ 0 & 0 & 0 \end{pmatrix}, \tag{6}$$

where the $\left(\begin{smallmatrix} a & b & c \\ 0 & 0 & 0 \end{smallmatrix}\right)$ are 3-j symbols. The radial integrals R_K are defined in Sec. III.

B. $(2p)^{-1}(3p)^{-n}\rightarrow(3s)^{-1}(3p)^{-(n+1)}[L_{2,3}\text{-}M_1M_{2,3}]$ transitions

The Auger rate for transitions of the type

$$(n_1l_1)[(n_4l_4)^p, S_4L_4]SL \rightarrow (n_3l_3)[(n_4l_4)^{p+1}, Q_4P_4]QP$$

is[1,8]

$$W_{fi}(LS,PQ)=(2P+1)(2Q+1)\prod_{i=1}^{4}(2l_i+1)(p+1)\sum_{P_4Q_4}(2P_4+1)(2Q_4+1)(l_4^{p+1}\beta_4P_4Q_4\{|l_4^p\alpha_4L_4S_4)^2$$
$$\times\left|\sum_{f,g}(-1)^f I(KK'fg)(2f+1)(2g+1)\begin{Bmatrix} P & g & L_4 \\ l_1 & L & l_2 \end{Bmatrix}\begin{Bmatrix} g & l_4 & l_3 \\ P_4 & P & L_4 \end{Bmatrix}\begin{Bmatrix} Q & f & S_4 \\ \frac{1}{2} & S & \frac{1}{2} \end{Bmatrix}\begin{Bmatrix} f & \frac{1}{2} & \frac{1}{2} \\ Q_4 & Q & S_4 \end{Bmatrix}\right|^2, \tag{7}$$

where the subscripts to the quantum numbers denote shells identified in Fig. 1.

C. $(2p)^{-1}(3p)^{-n}\rightarrow(3s)^{-2}(3p)^{-n}[L_{2,3}\text{-}M_1M_1]$ transitions

For this class of transitions, which accounts for only ~2% of the 2p Auger width, we neglect the effect of the partially filled 3p shell and compute the Auger rate in the traditional manner.[9]

III. RADIATIONLESS TRANSITION PROBABILITIES IN TERMS OF RADIAL MATRIX ELEMENTS

The Auger transition probabilities for each initial multiplet state were calculated, in terms of radial matrix elements, with the aid of a computer program that includes 3-j and 6-j symbol subroutines.

The radial integrals are

$$R_K(n_1l_1, n_2l_2, n_3l_3, n_4l_4)\equiv R_K(l_1l_2l_3l_4)$$
$$=\int_{r_1,r_2=0}^{\infty} r_1^2r_2^2\gamma_K R_{n_1l_1}(r_1)R_{n_2l_2}(r_2)$$
$$\times R_{n_3l_3}(r_1)R_{n_4l_4}(r_2)\,dr_1\,dr_2, \tag{8}$$

where

$$\gamma_K=\begin{cases} r_1^K/r_2^{K+1}, & r_1<r_2 \\ r_2^K/r_1^{K+1}, & r_1>r_2 \end{cases} \tag{9}$$

and the subscripts 1...4 pertain to the states identified in Fig. 1.

Results for atoms with one to five holes in the 3p shell are listed in Tables I–V. For the case of an empty 3p level (six holes), the familiar closed-shell results apply.[10]

IV. SUM RULES

For $(2p)^{-1}(3p)^{-n}\rightarrow(3p)^{-(n+2)}$ transitions, we find

$$\overline{W}_{fi}=\frac{\sum_{L_3,S_3}\sum_{P,Q}\sum_{L,S}(2L+1)(2S+1)W_{fi}[(L_3S_3)LS,PQ]}{(4l_1+2)[\sum_{L_3S_3}(2L_3+1)(2S_3+1)]}=\frac{(4l_3+2-n)(4l_3+1-n)}{(4l_3+2)(4l_3+1)}I_0, \tag{10}$$

where

TABLE III. Auger transition probabilities to an initial $2p$ vacancy in an atom with the electron configuration $(1s)^2(2s)^2(2p)^5(3s)^2(3p)^3$, for various initial multiplet states. Results are given in terms of radial integrals $R_K(l_1l_2l_3l_4)$ as defined in Eq. (8).

Multiplet state	Auger transition probability
$(^4S)^3P$	$\frac{1}{9}R_1(1100)^2+\frac{8}{3}[R_0(1111)-\frac{1}{5}R_2(1111)]^2+\frac{1}{9}R_1(1001)^2-\frac{8}{9}R_1(1001)R_0(1010)+\frac{8}{3}R_0(1010)^2+\frac{2}{9}R_1(1201)^2-\frac{16}{45}R_1(1201)R_2(1210)+\frac{16}{75}R_2(1210)^2$
$(^4S)^5P$	$\frac{1}{9}R_2(1100)^2+\frac{1}{9}R_1(1001)^2+\frac{2}{9}R_1(1201)^2$
$(^2P)^1S$	$\frac{1}{9}R_1(1100)^2+8[R_0(1111)-\frac{1}{5}R_2(1111)]^2+\frac{2}{9}R_1(1001)^2-\frac{8}{3}R_1(1001)R_0(1010)+8R_0(1010)^2+\frac{1}{9}R_1(1201)^2-\frac{4}{15}R_1(1201)R_2(1210)+\frac{4}{25}R_2(1210)^2$
$(^2P)^1P$	$\frac{1}{9}R_1(1100)^2+\frac{9}{50}R_2(1111)^2+\frac{1}{6}R_1(1001)^2+\frac{1}{6}R_1(1201)^2-\frac{1}{5}R_1(1201)R_2(1210)+\frac{3}{25}R_2(1210)^2$
$(^2P)^1D$	$\frac{1}{9}R_1(1100)^2+2[R_0(1111)-\frac{1}{50}R_2(1111)]^2+\frac{27}{625}R_2(1311)^2+\frac{1}{18}R_1(1001)^2-\frac{2}{3}R_1(1001)R_0(1010)+2R_0(1010)^2+\frac{5}{18}R_1(1201)^2-\frac{23}{75}R_1(1201)R_2(1210)+\frac{23}{125}R_2(1210)^2$
$(^2P)^3S$	$\frac{1}{9}R_1(1100)^2+\frac{2}{9}R_1(1001)^2+\frac{1}{9}R_1(1201)^2$
$(^2P)^3P$	$\frac{1}{9}R_1(1100)^2+\frac{1}{2}[2R_0(1111)+\frac{1}{5}R_2(1111)]^2+\frac{1}{6}R_1(1001)^2-\frac{2}{3}R_1(1001)R_0(1010)+2R_0(1010)^2+\frac{1}{6}R_1(1201)^2-\frac{1}{15}R_1(1201)R_2(1210)+\frac{1}{25}R_2(1210)^2$
$(^2P)^3D$	$\frac{1}{9}R_1(1100)^2+\frac{81}{1250}R_2(1111)^2+\frac{27}{625}R_2(1311)^2+\frac{5}{18}R_1(1201)^2-\frac{3}{25}R_1(1201)R_2(1210)+\frac{9}{125}R_2(1210)^2+\frac{1}{18}R_1(1001)^2$
$(^2D)^1P$	$\frac{1}{9}R_1(1100)^2+\frac{27}{250}R_2(1111)^2+\frac{1}{18}R_1(1201)+\frac{9}{125}R_2(1210)^2+\frac{5}{18}R_1(1001)^2-\frac{3}{25}R_1(1201)R_2(1210)$
$(^2D)^1D$	$\frac{1}{9}R_1(1100)^2+\frac{3}{2}[2R_0(1111)-\frac{7}{25}R_2(1111)]^2+\frac{9}{625}R_2(1311)^2+1.6R_1(1201)^2-\frac{7}{25}R_1(1201)R_2(1210)+\frac{21}{125}R_2(1210)^2+\frac{1}{6}R_1(1001)^2-2R_1(1001)R_0(1010)+6R_0(1010)^2$
$(^2D)^1F$	$\frac{1}{9}R_1(1100)^2+\frac{72}{875}R_2(1311)^2+\frac{1}{3}R_1(1201)^2-\frac{8}{25}R_1(1201)R_2(1210)+\frac{24}{125}R_2(1210)^2$
$(^2D)^3P$	$\frac{1}{9}R_1(1100)^2+\frac{5}{6}[-2R_0(1111)+\frac{1}{25}R_2(1111)]^2+\frac{5}{18}R_1(1001)^2-\frac{10}{9}R_1(1001)R_0(1010)+\frac{10}{3}R_0(1010)^2+\frac{1}{90}R_1(1201)^2-\frac{1}{225}R_1(1201)R_2(1210)+\frac{1}{375}R_2(1210)^2$
$(^2D)^3D$	$\frac{1}{9}R_1(1100)^2+\frac{27}{1250}R_2(1111)^2+\frac{9}{625}R_2(1311)^2+\frac{1}{6}R_1(1201)^2-\frac{1}{25}R_1(1201)R_2(1210)+\frac{3}{125}R_2(1210)^2+\frac{1}{6}R_1(1001)^2$
$(^2D)^3F$	$\frac{1}{9}R_1(1100)^2+\frac{72}{875}R_2(1311)^2+\frac{1}{3}R_1(1201)^2-\frac{4}{25}R_1(1201)R_2(1210)+\frac{12}{125}R_2(1210)^2$

$$I_0=\frac{1}{2}\,\frac{(2l_3+1)\prod_{i=1}^{3}(2l_i+1)}{4l_1+2}\sum_{f,g}(2f+1)(2g+1)I(KK'fg)^2 \tag{11}$$

is the full-shell rate.

The corresponding sum rule for $(2p)^{-1}(3p)^{-n}\rightarrow(3s)^{-1}(3p)^{-(n+1)}$ transitions has been derived by McGuire[1]:

$$\sum_{L,S,P_4,Q_4,P,Q}W_{fi}(LS,PQ)=\prod_{i=1}^{4}\frac{(2l_i+1)(4l_4+2-p)}{(4l_1+2)(4l_4+2)}\sum_{f,g}(2f+1)(2g+1)I(KK'fg)^2=\frac{4l_4+2-p}{4l_4+2}I_0, \tag{12}$$

where the full-shell rate is

$$I_0=\prod_{i=1}^{4}\frac{(2l_i+1)}{4l_1+2}\sum_{f,g}(2f+1)(2g+1)I(KK'fg)^2. \tag{13}$$

Equations (10) and (12) were used to check both algebraic and numerical results of the present work.

In the case of multiplets which occur twice or three times, the eigenfunctions were written as a linear combination of the terms of different parentage. For example, the wave functions for the ^2P multiplet in $(2p)^{-1}(3p)^{-2}$ configurations are

TABLE IV. Auger transition probabilities to an initial $2p$ vacancy in an atom with the electron configuration $(1s)^2(2s)^2(2p)^5(3s)^2(3p)^2$, for various initial multiplet states. Results are given in terms of radial integrals $R_K(l_1l_2l_3l_4)$ as defined in Eq. (8).

Multiplet state	Auger transition probability
$({}^1S)^2P$	$\frac{1}{9}R_1(1100)^2+\frac{1}{3}[R_0(1111)+\frac{2}{5}R_2(1111)]^2$ $+\frac{4}{54}R_1(1001)^2-\frac{2}{9}R_1(1001)R_0(1010)$ $+\frac{2}{3}R_0(1010)^2+\frac{4}{27}R_1(1201)^2-\frac{4}{45}R_1(1201)R_2(1210)$ $+\frac{4}{75}R_2(1210)^2$
$({}^3P)^2S$	$\frac{1}{9}R_1(1100)^2$
$({}^3P)^2P$	$\frac{1}{9}R_1(1100)^2+3[-R_0(1111)+\frac{1}{5}R_2(1111)]^2$ $+\frac{2}{9}R_1(1001)^2-2R_1(1001)R_0(1010)+6R_0(1010)^2$ $+\frac{1}{9}R_1(1201)^2-\frac{1}{5}R_1(1201)R_2(1210)$ $+\frac{3}{25}R_2(1210)^2$
$({}^3P)^2D$	$\frac{1}{9}R_1(1100)^2+\frac{1}{5}R_1(1201)^2-\frac{9}{25}R_1(1201)R_2(1210)$ $+\frac{27}{125}R_2(1210)^2$
$({}^3P)^4S$	$\frac{1}{9}R_1(1100)^2$
$({}^3P)^4P$	$\frac{1}{9}R_1(1100)^2+\frac{2}{9}R_1(1001)^2+\frac{1}{9}R_1(1201)^2$
$({}^3P)^4D$	$\frac{1}{9}R_1(1100)^2+\frac{1}{5}R_1(1201)^2$
$({}^1D)^2P$	$\frac{1}{9}R_1(1100)^2+\frac{5}{3}[R_0(1111)+\frac{1}{25}R_2(1111)]^2$ $+\frac{10}{27}R_1(1001)^2-\frac{10}{9}R_1(1001)R_0(1010)$ $+\frac{10}{3}R_0(1010)^2+\frac{1}{135}R_1(1201)^2$ $-\frac{1}{225}R_1(1201)R_2(1210)+\frac{1}{375}R_2(1210)^2$
$({}^1D)^2D$	$\frac{1}{9}R_1(1100)^2+\frac{1}{15}R_1(1201)^2$ $-\frac{1}{25}R_1(1201)R_2(1210)+\frac{3}{125}R_2(1210)^2$
$({}^1D)^2F$	$\frac{1}{9}R_1(1100)^2+\frac{54}{875}R_2(1311)^2$ $+\frac{4}{15}R_1(1201)^2-\frac{4}{25}R_1(1201)R_2(1210)$ $+\frac{12}{125}R_2(1210)^2$

$$
\begin{aligned}
\psi^{(1)}({}^2P) &= c_0\psi[({}^1S)^2P]+c_1\psi[({}^3P)^2P]+c_2\psi[({}^1D)^2P]\,,\\
\psi^{(2)}({}^2P) &= c_0'\psi[({}^1S)^2P]+c_1'\psi[({}^3P)^2P]+c_2'\psi[({}^1D)^2P]\,, \qquad (14)\\
\psi^{(3)}({}^2P) &= c_0''\psi[({}^1S)^2P]+c_1''\psi[({}^3P)^2P]+c_2''\psi[({}^1D)^2P]\,.
\end{aligned}
$$

The mixing coefficients were found by diagonalizing the energy matrix.[11] The two-electron Slater integrals needed in the calculation of the energy matrix elements were taken from Mann's work for neutral atoms.[12] These mixed-parentage eigenfunctions were used for the Auger transition-probability calculations for multiplets which occur more than once.

TABLE V. Auger transition probabilities to an initial $2p$ vacancy in an atom with the electron configuration $(1s)^2(2s)^2(2p)^5(3s)^2(3p)$, for various initial multiplet states. Results are given in terms of radial integrals $R_K(l_1l_2l_3l_4)$ as defined in Eq. (8).

Multiplet state	Auger transition probability
${}^1S$	$\frac{1}{9}R_1(1100)^2+3[-\frac{1}{3}R_1(1001)+2R_0(1010)]^2$
${}^1P$	$\frac{1}{9}R_1(1100)^2$
${}^1D$	$\frac{1}{9}R_1(1100)^2+\frac{6}{5}[\frac{1}{3}R_1(1201)-\frac{2}{5}R_2(1210)]^2$
${}^3S$	$\frac{1}{9}R_1(1100)^2+\frac{1}{3}R_1(1001)^2$
${}^3P$	$\frac{1}{9}R_1(1100)^2$
${}^3D$	$\frac{1}{9}R_1(1100)^2+\frac{2}{15}R_1(1201)^2$

V. TRANSITION RATES AND FLUORESCENCE YIELDS

Radial matrix elements were calculated from Hartree-Fock-Slater one-electron radial eigenfunctions with $X\alpha$ exchange. The α parameters were taken from Schwarz's work pertaining to neutral atoms.[13] The change in α caused by ionization in an outer shell is very small,[14] so that the same α could be used for all configurations considered in this paper. The wave functions were generated using the appropriate potential for each individual defect configuration. The frozen-orbitals approximation was used, assuming that the initial and final one-electron wave functions are the same.

X-ray and Auger energies for the various configurations were taken from the work of Larkins,[15] who used the Hartree-Fock approach to calculate the total energy difference in adiabatic approximation.

The radiative transition rates, in dipole approximation, are the same for the various multiplet states of each initial hole configuration if multiplet energy splitting (approximately 2 eV out of 240 eV) is neglected (Table VI).

Auger rates to the $2p$ hole and $L_{2,3}$ fluorescence

TABLE VI. Argon $2p$ radiative widths (in multiples of 10^{-7} a.u.) for various initial hole configurations.

Initial configuration	Radiative width
$(2p)^{-1}$	8.633
$(2p)^{-1}(3p)^{-1}$	8.788
$(2p)^{-1}(3p)^{-2}$	9.558
$(2p)^{-1}(3p)^{-3}$	10.425
$(2p)^{-1}(3p)^{-4}$	11.389
$(2p)^{-1}(3p)^{-5}$	12.46
$(2p)^{-1}(3p)^{-6}$	13.24

TABLE VII. Radiationless transition probabilities (in multiples of 10^{-3} a.u.) and fluorescence yields (in multiples of 10^{-4}) for an Ar $2p$ vacancy in the presence of a partially filled $3p$ shell, for given initial multiplet states.

Initial hole configuration	Initial multiplet term	Auger rate	Fluorescence yield
$(2p)^{-1}(3p)^{-1}$	^1S	9.210	0.954
	^1P	0.479	18.34
	^1D	10.235	0.859
	^3S	0.133	66.15
	^3P	10.906	0.806
	^3D	0.347	25.31
$(2p)^{-1}(3p)^{-2}$	$^2P^{(1)}$	9.556	1.000
	$^2P^{(2)}$	3.38	2.828
	$^2P^{(3)}$	1.686	5.669
	$(^3P)^2S$	0.544	17.566
	$^2D^{(1)}$	14.690	0.651
	$^2D^{(2)}$	0.481	19.832
	$(^3P)^4S$	15.859	0.603
	$(^3P)^4P$	0.150	63.635
	$(^3P)^4D$	0.285	33.56
	$(^1D)^2F$	0.2676	35.717
$(2p)^{-1}(3p)^{-3}$	$^3P^{(1)}$	15.393	0.6773
	$^3P^{(2)}$	1.938	5.376
	$^3P^{(3)}$	0.339	30.640
	$(^4S)^5P$	0.169	61.686
	$(^2P)^1S$	15.580	0.669
	$^1P^{(1)}$	0.128	81.04
	$^1P^{(2)}$	0.535	19.434
	$^1D^{(1)}$	16.593	0.628
	$^1D^{(2)}$	0.3224	32.231
	$(^2P)^3S$	0.254	41.043
	$^3D^{(1)}$	0.169	61.417
	$^3D^{(2)}$	0.315	32.976
	$(^2D)^1F$	0.228	45.724
	$(^2D)^3F$	0.228	45.724
$(2p)^{-1}(3p)^{-4}$	$^2P^{(1)}$	15.568	0.732
	$^2P^{(2)}$	1.466	7.769
	$^2P^{(3)}$	0.4581	24.861
	$(^3P)^2S$	0.0909	125.28
	$^2D^{(1)}$	0.0912	124.88
	$^2D^{(2)}$	0.0912	124.88
	$(^3P)^4S$	0.0909	125.28
	$(^3P)^4P$	0.281	40.52
	$(^3P)^4D$	0.0920	123.79
	$(^1D)^2F$	0.212	53.80
$(2p)^{-1}(3p)^{-5}$	^1S	12.25	1.017
	^1P	0.0994	123.81
	^1D	0.0995	123.68
	^3S	0.412	30.14
	^3P	0.0994	123.81
	^3D	0.1002	122.82
$(2p)^{-1}(3p)^{-6}$	^2P	0.1093	121.48

TABLE VIII. Argon average $L_{2,3}$ fluorescence yields (in multiples of 10^{-4}) for various $(2p)^{-1}(3p)^{-n}$ configurations.

Initial hole configuration	$2p$ fluorescence yield
$(2p)^{-1}$	1.48
$(2p)^{-1}(3p)^{-1}$	17.97
$(2p)^{-1}(3p)^{-2}$	24.83
$(2p)^{-1}(3p)^{-3}$	37.84
$(2p)^{-1}(3p)^{-4}$	79.61
$(2p)^{-1}(3p)^{-5}$	112.16
$(2p)^{-1}(3p)^{-6}$	121.48

yields for the various initial multiplet states are summarized in Table VII. Average fluorescence yields for each hole configuration, computed according to Eq. (1), are listed in Table VIII.

VI. COMPARISON WITH EXPERIMENT

These calculations were performed for the specific case of the Ar $2p$ fluorescence yield in the presence of $3p$ vacancies because Fortner[6,16] has recently made a comprehensive set of measurements on this system. L x rays emitted in Ar + Ar collisions at various energies were analyzed with a Bragg spectrometer, and the unfolded peaks were correlated with various vacancy states on the basis of adiabatic Hartree-Fock calculations of energy shifts.[6] Fortner noted that in most cases more than 90% of the observed x rays were from $3s \rightarrow 2p$ transitions in atoms with a single L vacancy. Fortner derived experimental fluorescence yields by dividing the measured x-ray production cross sections by total L-shell ionization cross sections $\sigma_I = 2\pi r_x^2$, where r_x is the level-crossing radius. The measured fluorescence yields can be compared with theoretical results through the relation

$$(\bar{\omega})^{-1} = \Sigma (N_i/\omega_i), \tag{15}$$

where N_i is the fractional x-ray yield corresponding to vacancy configuration i with fluorescence yield ω_i.

Uncertainties in the analysis arise from the deconvolution of the x-ray spectra, from the fact that $3s$ and $3p$ vacancies could not be distinguished with the available spectrometer resolution, and from some degeneracy between transitions to double and single L vacancies. Fortner showed that Eq. (15), with traditionally computed theoretical fluorescence yields for various M-shell defect configurations,[3,4,17] leads to results that fall below measured fluorescence yields by a factor of ~4.4 (Fig. 2).

The present calculation leads to considerably better agreement with experiment, as illustrated

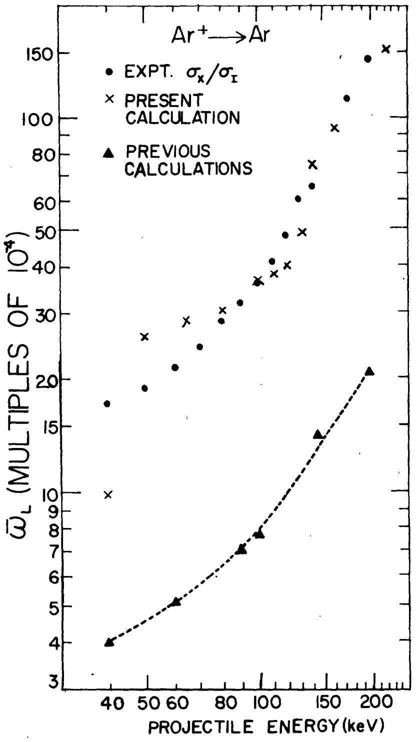

FIG. 2. Measured effective argon L fluorescence yields, $\bar{\omega}_L = \sigma_x/\sigma_I$, as a function of bombarding energy, after Ref. 6. Calculated yields based on Refs. 3, 4, and 13 fall near the dashed curve, which represents the measurements divided by 4.4 (Ref. 6). The crosses indicate calculations from yields for individual initial-state multiplet configurations (Table VIII).

in Fig. 2. Here we have taken Fortner's analysis[6] of L x rays from $Ar^+ + Ar$ collisions at various energies and computed effective fluorescence yields with the theoretical results of Table VIII. For projectile energies below 130 keV, we assumed that only single $2p$ vacancies were created in the collisions, because at these energies Fortner's spectra[6] do not show the signature of double L-hole events, viz., (i) x rays shifted ~25 eV up from transitions to a single L vacancy in the presence of n $3p$ holes, *and* (ii) x rays that correspond to a single L vacancy in the presence of $n+2$ $3p$ holes. At bombarding energies of 130 keV and above, there is evidence for the production of double L vacancies, and we have multiplied the calculated effective fluorescence yields by a factor of 1.4 to account for this effect, as suggested by Fortner.[6]

Except at 40 keV, calculated and measured fluorescence yields agree to better than 30%. The calculated yield at 40 keV would agree much better with experiment if the number of L x rays emitted by Ar atoms without any $3p$ vacancies were somewhat smaller than the 9% indicated by Fortner's analysis.

The results of the present calculations can also be tested by comparison with the measured effective L fluorescence yield[6] in 90 keV $Ar^+ \rightarrow CH_4$ collisions, which is 19×10^{-4}. Using Fortner's analysis which indicates that 68% of the x rays originate from Ar atoms with one $3p$ vacancy and 20% from Ar atoms with two $3p$ vacancies, and not including the 12% of unidentified x rays above 253 eV, we find from Table VIII a calculated value of $\omega_L = 21.42\times10^{-4}$.

The discrepancies that remain may, at least in part, be due to the experimental uncertainties discussed above and to the fact that the various initial multiplet states may not always be populated statistically in collision events.[18]

ACKNOWLEDGMENTS

We are much indebted to Dr. E. J. McGuire of the Sandia Laboratories and Dr. R. J. Fortner of the Lawrence Livermore Laboratory for communicating their results to us in advance of publication. We thank Dr. C. P. Bhalla for a helpful comment regarding the mixing of multiplet states of different parentage. It is a pleasure to acknowledge helpful conversations with Dr. D. A. Ringers.

---

†Research supported in part by the U.S. Army Research Office-Durham and by the National Aeronautics and Space Administration (Grant NGR 38-003-036).

*A preliminary report on this work was presented at the International Conference on X-Ray Processes in Matter, Otaniemi, Finland, 1974. M. H. Chen and B. Crasemann, Physica Fennica 9, S1, 250 (1974).

[1] E. J. McGuire, Phys. Rev. A 10, 32 (1974).

[2] C. P. Bhalla, Phys. Lett. 46A, 185 (1973).

[3] F. P. Larkins, J. Phys. B 4, L29 (1971).

[4] C. P. Bhalla and D. L. Walters, in *Proceedings of the International Conference on Inner-Shell Ionization Phenomena*, edited by R. W. Fink, S. T. Manson, J. M. Palms, and P. Venugopala Rao, U.S. AEC Report No. CONF-720404 (U.S. GPO, Washington, D.C., 1973), p. 1572.

[5] V. R. Veluri, F. E. Wood, J. M. Palms, and P. Venugopala Rao, in Ref. 4, p. 251.

[6] R. J. Fortner, preceding paper, Phys. Rev. A 10, 2218 (1974).

[7] E. J. McGuire, in *Atomic Inner-Shell Processes*, edited by B. Crasemann (Academic, New York, to be published).

[8] This expression differs by $(2\pi)^{-1}$ from the result given in Ref. 1, because our normalization of the continuum state differs from McGuire's by 2π.

[9] M. H. Chen, B. Crasemann, and V. O. Kostroun, Phys. Rev. A 4, 1 (1971).

[10] R. A. Rubenstein, thesis (University of Illinois, 1955) (unpublished).

[11] J. C. Slater, *Quantum Theory of Atomic Structure* (McGraw-Hill, New York, 1960), Vol. II.

[12] J. B. Mann, Los Alamos Scientific Laboratory Report No. LA-3690, 1967 (unpublished).

[13] K. Schwarz, Phys. Rev. B 5, 2466 (1972).

[14] D. A. Ringers and M. H. Chen (unpublished).

[15] F. P. Larkins, J. Phys. B 4, 1 (1971).

[16] R. J. Fortner, Bull. Am. Phys. Soc. 18, 1575 (1973).

[17] C. P. Bhalla, in Proceedings of the Fifth International Conference on Atomic Collisions in Solids, Gatlinburg, Tennessee, September 1973 (unpublished).

[18] C. P. Bhalla, D. L. Matthews, and C. F. Moore, Phys. Lett. 46A, 336 (1974).